diffraction structural biology

A degradation signal recognition in prokaryotes

Eun Young Park and Hyun Kyu Song*

School of Life Sciences and Biotechnology, Korea University, Seoul 136-701, Republic of Korea.
E-mail: hksong@korea.ac.kr

The degradation of ssrA-tagged substrates in prokaryotes is conducted by a subset of ATP-dependent proteases, including ClpXP complex. More than 630 sequences of ssrA have been identified from 514 species, and are conserved in a wide range of prokaryotes. SspB protein markedly stimulates the degradation of these ssrA-tagged substrates by the ClpXP proteolytic machine. The dimeric SspB protein is composed of a compact ssrA-binding domain, which has a dimerization surface and a flexible C-terminal tail with a ClpX-binding motif at its very end. Since SspB is an adaptor protein for the ClpXP complex, designed mutagenesis, fluorescence spectroscopy, biochemistry and X-ray crystallography have been used to investigate the mechanism of delivery of ssrA-tagged proteins. In this paper the structural basis of ssrA-tag recognition by ClpX and SspB, as well as SspB-tail recognition by ZBD, is described.

1. Introduction

Energy-dependent proteases play pivotal roles in the quality control of eukaryotic and prokaryotic cells (Goldberg, 1990; Gottesman, 1996; Wickner et al., 1999). The ATP-dependent 26S proteasome is a master player in intracellular protein degradation in eukaryotes (Goldberg, 2003; Pines & Lindon, 2005), while several ATP-dependent proteases including ClpXP, ClpAP and HslVU perform similar tasks in prokaryotes (Gottesman, 1996; Sauer et al., 2004; Bochtler et al., 1999). These two-component systems consist of a proteolytic core (ClpP, HslV and 20S proteasome) and an activator (ClpX, ClpA, HslU and 19S regulatory particle). The protease activity is tightly coupled with the ATPase/unfoldase activity of its activator component. These ATPases are members of the Hsp100 family and form hexameric ring-shaped structures with a narrow translocation channel in the center (Hanson & Whiteheart, 2005; Bochtler et al., 2000; Beuron et al., 1998; Kessel et al., 1996) (Fig. 1a). The ATPase core shares significant sequence similarity (typical AAA-ATPase); however, the accessory parts for substrate recognition differ markedly (Mogk et al., 2004; Song et al., 2000).

In eukaryotes, the lid of the 19S regulatory cap recognizes ubiquitin chains that are covalently attached to a specific lysine residue in the substrates (Hershko & Ciechanover, 1998). No similar tagging system has been found in prokaryotes. One well characterized system in prokaryotes is an 11 amino acid residue peptide known as ssrA (AANDENYALAA; Escherichia coli sequence), which specifically directs the marked substrates to the ClpXP or ClpAP proteases (Gottesman et al., 1998; Withey & Friedman, 2002) (Fig. 2a). This ssrA tag is encoded by a unique tmRNA that possesses the features of both transfer RNA and messenger RNA, and is attached to the C-terminus of nascent polypeptides on the stalled ribosome (Keiler et al., 1996). More than 630 ssrA sequences encoded by tmRNA have been reported from over 510 species across 17 phyla (the tmRNA site: http://www.indiana.edu/~tmrna/). ClpX and ClpA both recognize ssrA-tagged proteins, but they show distinct positional preferences on

the ssrA tag (Flynn et al., 2001) (Fig. 2a). The degradation of ssrA-tagged substrates by ClpXP is markedly enhanced by an adaptor protein SspB (stringent starvation protein B), which also binds specifically to ssrA tag (Song & Eck, 2003; Levchenko et al., 2000, 2003). Interestingly, the binding determinant in the ssrA tag for SspB and ClpA shows partial overlap, and therefore SspB inhibits the degradation of substrates by ClpAP complex (Flynn et al., 2001).

The SspB protein is composed of a dimeric ssrA binding domain (Fig. 2c) and an unstructured C-terminal 50 residue tail (Song & Eck, 2003; Levchenko et al., 2003). Elegant engineering on SspB constructs with a heterodimer lacking a C-terminal tail suggests that both tails of SspB are required for strong binding to ClpX and efficient delivery of the ssrA-tagged substrates to the ClpXP degradation machine (Bolon et al., 2004). The extreme C-terminal segment of SspB (XB: ClpX-binding region) and the N-terminal domain of ClpX are crucial for tethering the delivery complex (Dougan et al., 2003; Wah et al., 2003). The N-terminal domain of ClpX is a C4-type zinc-binding domain (ZBD), and is responsible for the recognition of several target substrates, including MuA transposase, λO replication protein, and the UmuD′ subunit of error-prone DNA polymerase (Banecki et al., 2001; Levchenko et al., 1995; Frank et al., 1996). The solution structure of the ZBD from E. coli and the crystal structure of the ATPase domain from Helicobacter pyroli have been reported (Kim & Kim, 2003; Donaldson et al., 2003). The ZBD of ClpX is a stable dimer, whereas full-length ClpX is a hexamer (Fig. 1a). The ZBD is a separate domain from the hexameric AAA+ ring of ClpX (Fig. 1b) and undergoes large ATP-dependent block movement into the ATPase core (Thibault, Tsitrin et al., 2006). The SspB adaptor also modulates ZBD movement (Thibault, Tsitrin et al., 2006). The ClpX hexamer contains three XB binding sites, one per ZBD dimer, and thus binds strongly to just one SspB dimer at a time (Bolon et al., 2004).

Recently, the high-resolution structure of the ZBD in complex with XB peptide has been reported (Park et al., 2007). The dimeric ZBD structure with two independent XB peptides contrasts with the
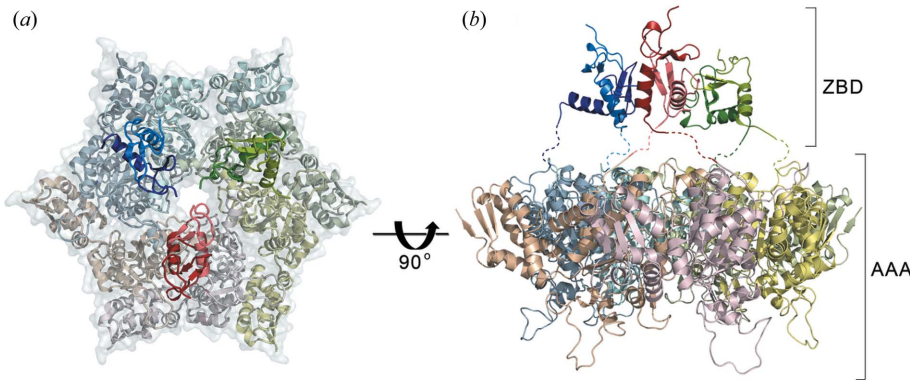
Figure 1
Schematic model of the full-length ClpX hexamer. A monomeric model of the ATPase domain of *E. coli* ClpX has been generated with that of *H. pylori* ClpX [Protein Data Bank (PDB) ID: 1UM8] using the SWISS-MODEL server (Schwede *et al.*, 2003) initially. The hexameric model has been generated with the guidance of HslU hexamer (PDB ID: 1E94), and the resulting model was energetically minimized using *CNS* software (Brunger *et al.*, 1998). Although the exact orientation of ZBD is ambiguous, their location is distal to the ATPase domain (AAA+ ring) of ClpX based on earlier electron microscopic images (Grimaud *et al.*, 1998), as well as the direction of each chain terminus (N-terminus for the polypeptide chain of ATPase domain and C-terminus for that of ZBD). (*a*) Top view showing the hexameric pore in the center. The ZBD is drawn with ribbon and the ATPase domain (AAA) with ribbon plus transparent molecular surface, and the linker between the ATPase domain and ZBD is missing. (*b*) Side view [90° rotation of (*a*) along the horizontal axis] with the ZBD domain extending upward. The figure was drawn using *PyMOL* (http://www.pymol.org).
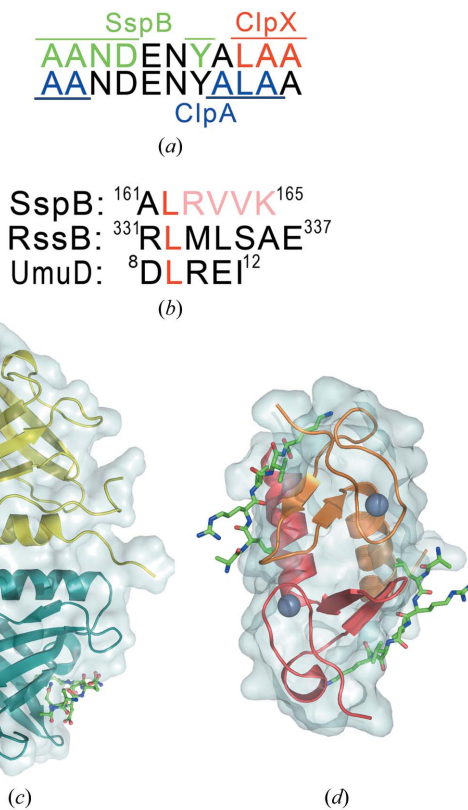
Figure 2
(*a*) Recognition determinants in the ssrA tag for ClpX (coloured red), SspB (green) and ClpA (blue). (*b*) Recognition determinants in the SspB tail for ZBD of ClpX and the conserved ZBD-interacting determinants in the ClpX interacting proteins, RssB and UmuD. Leucine residues (coloured red) are the key determinant. Other residues (pink) in SspB are also involved in the interaction with ZBD. (*c*) Structure of the SspB-ssrA complex. Ribbon diagram with transparent surface of dimeric SspB and stick model of ssrA peptides. The flexible C-terminal tail of SspB is invisible in the crystal structure (PDB ID: 1OX9). (*d*) Structure of ZBD-XB complex. Ribbon diagram with transparent surface of dimeric ZBD and stick model of SspB-tail peptides (PDB ID: 2DS8). The two slate-coloured balls are bound zinc atoms. The orientation of (*c*) and (*d*) is a view looking down at the twofold molecular symmetry. Parts (*c*) and (*d*) were also drawn using *PyMOL*.

reported stoichiometry of one XB peptide per ZBD dimer obtained using biochemical techniques (Bolon *et al.*, 2004). These results have suggested a plausible model of target substrate delivery to the ClpXP degradation machine (Park *et al.*, 2007). In this paper we describe the structural basis of ssrA-tag recognition by ClpX and SspB, as well as SspB-tail recognition by ZBD.

2. Degradation signal recognition

More than 50 potential ClpXP substrates have been revealed by the mass spectroscopic analysis of trapped substrates of the *E. coli* proteome using a histidine-tagged and inactive variant of ClpP (Flynn *et al.*, 2003). They are classified into at least five ClpX-recognizing motifs: three located at the N-terminus (N-motif 1: polar-T/φ-φ-basic φ; N-motif 2: NH$_2$-Met-basic φ-φ-φ; N-motif 3: φ-x-polar-x-polar-x-basic polar) and two at the C-terminus (C-motif 1: LAA-COOH, ssrA-type; C-motif 2: RRKKAI-COOH, MuA-type). Later, large peptide libraries were applied to identify the sequence recognition pattern by ZBD and the AAA+ ring separately (Thibault, Yudin *et al.*, 2006). ZBD and the AAA+ ring of ClpX preferentially bind to hydrophobic residues but have different sequence preferences, and ZBD has higher specificity in substrate selection than AAA+ domain, as expected.

2.1. SsrA recognition by ClpX and SspB

Elegant mutational analyses on the ssrA peptide with ClpX, ClpA and SspB revealed overlapping recognition determinants in ssrA tag (Flynn *et al.*, 2001). ClpX recognizes the last three residues (Leu9, Ala10 and Ala11) at the C-terminus of the ssrA tag, whereas ClpA interacts with residues 8–10 (Ala8, Leu9 and Ala10) and the first two residues (Ala1 and Ala2) at the N-terminus (Fig. 2*a*). Both Clp-family ATPases share the recognition determinants (Leu9 and Ala10), and ClpA probably has stronger affinity than ClpX, assuming that more residues of the ssrA tag are involved in the recognition (Fig. 2*a*). Although ClpX alone is able to interact with the ssrA-tagged substrates and delivers them to ClpP protease, the adaptor protein, SspB, markedly enhances the recognition of the ssrA tag (Levchenko *et al.*, 2000; Wojtyra *et al.*, 2003). In the SspB–ssrA complex structure (Fig. 2*c*) the ssrA peptide binds in an irregular conformation in a groove formed by several hydrophobic residues (Song & Eck, 2003).
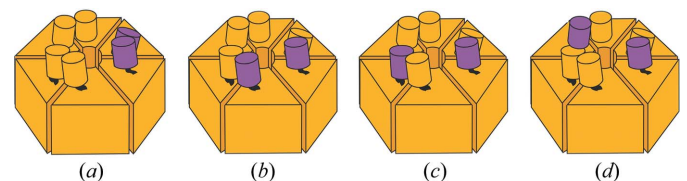
Figure 3
Schematic drawing of ClpX. The monomeric ATPase domain of ClpX is represented as a piece of the hexagonal casket at the bottom. The monomeric N-terminal ZBD is a cylinder at the top. Each ZBD monomer contains a binding site for the SspB tail based on the crystal structure. Therefore, the purple-coloured pairs are all possible functional ZBD units for efficient delivery of ssrA-tagged substrates by SspB adaptor protein (*a*)–(*d*).

SspB recognizes residues 1–4 (Ala1, Ala2, Asn3, Asp4) and 7 (Tyr7), which are N-terminal to the ClpX determinants but overlap the ClpA determinants (Fig. 2a). As a result, SspB competes with ClpA on the ssrA-tagged substrate, but SspB and ClpX work together to recognize them efficiently. The interaction between SspB and ssrA buries approximately 1180 Å^2 of solvent-accessible surface (Song & Eck, 2003). The first two alanine residues in ssrA fit well into the shallow hydrophobic depressions that do not readily accommodate bulkier side-chains. Side-chain atoms of Asn3 and Asp4 in the ssrA peptide form hydrogen bonds with the main-chain atoms of Asn54 and Gly78 in SspB, respectively. Glu5 in ssrA extends into the basic pocket formed by two arginine residues (Arg58 and Arg96) in SspB, but peptide array results show that this position is not critical (Flynn et al., 2001). Tyr7 in ssrA contributes numerous van der Waals interactions (Song & Eck, 2003). The carbonyl oxygen of Ala8 in ssrA forms hydrogen bonds with the guanidium moiety of Arg75 in SspB. The last three C-terminal residues (Leu9, Ala10 and Ala11) are recognized by ClpX as noted above, but detailed structural information is not available. Instead, manipulations of these residues, including DAS and LDD mutations, have been performed to investigate the importance of the residues (McGinness et al., 2006). These modified ssrA tags have weakened interactions with ClpXP. ClpXP degrades the substrates bearing these engineered peptide tags up to 100-fold differently, depending on the presence or absence of SspB protein (McGinness et al., 2006).

The SspB adaptor also binds peptide sequences in the stress-response regulator, RseA (Flynn et al., 2004). Interestingly, the RseA is located in the same peptide-binding groove of SspB, but the orientation of the RseA peptide is opposite in direction to the ssrA peptide (Levchenko et al., 2005). One similar example is that both orientations of left-handed helical polyproline II conformations of the proline-rich sequence are promiscuously recognized by SH3 domain (Mayer & Eck, 1995). Thus, the SspB adaptor protein has a highly versatile mode of target recognition and dynamic substrate delivery (Levchenko et al., 2005). Recently, an ortholog of SspB in Caulobacter crescentus, an α-proteobacterium, was identified (Lessner et al., 2007; Chien, Perchuk et al., 2007). C. crescentus SspB has limited sequence similarity with E. coli SspB, and the ssrA sequence of C. crescentus (AANDNFAEEFAVAA) is different in many positions as well as its length (Lessner et al., 2007), so studies on this complex should provide new insights into ssrA/adaptor protein interactions.

2.2. SspB-tail recognition by ZBD

Adaptor molecules are necessary for efficient delivery of substrates to ClpXP in many cases (Flynn et al., 2004; Neher, Sauer et al., 2003; Neher, Flynn et al., 2003). SspB enhances the delivery of ssrA-tagged substrates (C-motif 1) and RseA to ClpXP complex (Levchenko et al., 2000; Flynn et al., 2004). RssB delivers σ^S (N-motif 1) to ClpXP (Becker et al., 1999; Zhou et al., 2001) and UmuD confers instability on UmuD′ (Frank et al., 1996). Although the sequences among these adaptors do not align well, a similar motif (156-GGRPA**L**RVVK-165 in SspB; 327-GGRLR**L**MLSAE-337 in RssB, 8-D**L**REI-12 in UmuD), especially the leucine residue (boldface), is required for the interaction with ZBD (Dougan et al., 2003; Wah et al., 2003; Neher, Sauer et al., 2003) (Fig. 2b). The side-chain of this Leu161 in SspB extends into the favourable hydrophobic pocket formed by Phe16, Leu42 and Ile46 in ZBD (Park et al., 2007). Previous mutational studies on this residue are consistent with the structural information (Dougan et al., 2003; Wah et al., 2003). The critical role of Leu9 in UmuD has also been previously reported

(Neher, Sauer et al., 2003), and the importance of Leu332 in RssB should be confirmed. Our binding constant measurement derived from the calorimetric method showed that the upper conserved sequence GG(R/K) in SspB and RssB does not contribute to the affinity between the adaptor molecule and ZBD (data not shown). Pro159 and Ala160 in SspB are also not involved in the interaction between the SspB tail and ZBD.

Besides the key hydrophobic interaction by Leu161, other interactions are basically main-chain–main-chain interactions forming an antiparallel β-sheet and additional hydrophobic contacts. Although side-chain atoms of Arg162 in SspB do not participate in the interaction, main-chain atoms make critical hydrogen bonds with the backbone of Ala29 in ZBD. The hydrophobic side-chain of Val163 in SspB interacts with that of Ile46 in ZBD, and the side-chain of Val164 in SspB also interacts with the hydrophobic side-chains of Leu12 and Ala29 in ZBD. The C-termini Lys165 interacts with several residues in ZBD, including Gln21, Val24, Lys26 and Leu27 (Park et al., 2007). These interacting residues in ZBD revealed by the crystal structure are generally consistent with independent NMR titration experiments (Thibault, Yudin et al., 2006).

The DLREI segment of UmuD and RLMLSAE of RssB probably share the same ZBD binding site with SspB. λO peptide (residues 49–63) competes with the SspB tail to the binding site of ZBD (Thibault, Yudin et al., 2006). Although identifying a consensus sequence for a sequence-specific interaction is not straightforward, the main features of this ZBD binding motif are fully exposed hydrophobic residues (Fig. 2b). A peptide array experiment confirmed that ZBD preferentially binds to sequences enriched in both hydrophobic residues and the positively charged lysine. Interestingly, the ATPase domain of ClpX also prefers hydrophobic residues, but shows distinct sequence patterns (Thibault, Yudin et al., 2006).

2.3. SsrA-tagged substrate delivery by SspB

The dissociation constants for SspB proteins and XB peptides with the ZBD domain show approximately a tenfold difference, indicating the presence of two ClpX-binding tails of an SspB dimer that are able to interact with the ZBD domain simultaneously (Bolon et al., 2004). There are several proposed mechanisms of ssrA-tagged substrate delivery by SspB (Song & Eck, 2003; Dougan et al., 2003; Bolon et al., 2004; Thibault, Yudin et al., 2006). An arrangement where the twofold axis of SspB is aligned with the sixfold axis of ClpX, with the SspB dimer oriented such that the C-terminal LAA sequence of ssrA tag extends toward ClpX, makes sense given the observed 1:1 stoichiometric interaction between dimeric SspB and hexameric ClpX (Wah et al., 2002; Song & Eck, 2003). However, the symmetry may be broken when the ssrA-tagged substrate is delivered into a single pore of the AAA+ ring. Moreover, the dimeric ZBD undergoes large nucleotide-dependent movement relative to the AAA+ ring depending on the conformational status, capture versus feeding (Thibault, Tsitrin et al., 2006). An elegant protein design study showed that both SspB tails and their XB modules are required for efficient delivery, and isothermal titration calorimetry and fluorescence anisotropic spectroscopy revealed only one SspB-tail binding site in the ZBD dimer, providing a delivery complex model (Bolon et al., 2004). If only a single XB peptide binds to dimeric ZBD, the ClpX hexamer contains just three tethering sites for SspB, and one site is unoccupied when dimeric SspB engages hexameric ClpX to make an efficient delivery complex. The affinity of dimeric SspB to dimeric ZBD and the geometry of the SspB–ZBD complex were investigated using the quantitative optical biosensor method of dual polarization interferometry (Thibault, Yudin et al., 2006). Four binding modes of

dimeric SspB to the ZBD trimer of dimers have been proposed, with one being the most favourable mode of association: where one tail of SspB binds to the top of dimeric ZBD, whereas the other tail binds to the bottom of the second ZBD dimer. However, this model must be validated if two separate binding sites in dimeric ZBD are oriented differently to the AAA+ ring; one distal site to the AAA+ ring might be freely accessible by the SspB tail and the other proximal site might be blocked by the core AAA+ domain. Structural information of the full-length ClpX hexamer is needed to validate this model.

In contrast to previous models, the high-resolution electron density of the ZBD-XB complex suggests the presence of two separate SspB-tail binding sites in a dimeric ZBD (Park *et al.*, 2007). Therefore, there are in total six independent tethering sites in hexameric ClpX. Once a dynamic single tail of SspB binds to an XB binding site in the ZBD, subsequent interactions with the unoccupied five tethering sites are all possible theoretically, and thus roughly four different modes of association might be considered (Fig. 3); two in a ZBD dimer (Fig. 3*a*), each neighboring subunit in two ZBD dimers (Fig. 3*b*), one in a ZBD dimer and the other one subunit beyond the ZBD (Fig. 3*c*), and the other two subunits beyond the ZBD (Fig. 3*d*). There may be a preference for the second tethering site given distance and orientation restraints. Although the structure of a full-length ClpX has yet to be reported, the distance between the first and second binding site may be unattainable with the limited length of two SspB tails, and the orientation of the ZBD dimer in hexameric ClpX may affect the second molecular interaction. For example, one of the two binding sites in dimeric ZBD is pointing to the hexameric pore in the ATPase domain, and the other is pointing outside the molecule. Regardless of the orientation of the ZBD, the current structural data favour the model comprising a 1:1 complex between dimeric SspB and the ZBD (Fig. 3*a*). To support this model, we have designed an SspB–ClpX fusion chimera where all six XB binding sites in ZBD will be occupied by SspB tails. This variant possesses almost full proteolytic activity with a non-covalent SspB:ClpX complex (Park *et al.*, 2007). Although using the chimera cannot prove this mechanism because of differences in stoichiometry between SspB and ClpX, as well as no direct evidence that all six XB binding sites are occupied simultaneously, it insinuates that the ZBD dimer can be a functional unit for making an SspB:ClpXP delivery complex. A solid understanding of how ssrA-tagged substrates are delivered to the ClpXP degradation machine by SspB must await structural information of a complex between full-length SspB and ClpX.

Note added in proof. The structure of SspBα from *C. crescentus* in complex with ssrA tag has been reported in the middle of reviewing this manuscript (Chien, Grant *et al.*, 2007).

References

Banecki, B., Wawrzynow, A., Puzewicz, J., Georgopoulos, C. & Zylicz, M. (2001). *J. Biol. Chem.* **276**, 18843–18848.
Becker, G., Klauck, E. & Hengge-Aronis, R. (1999). *Proc. Natl. Acad. Sci. USA*, **96**, 6439–6444.
Beuron, F., Maurizi, M. R., Belnap, D. M., Kocsis, E., Booy, F. P., Kessel, M. & Steven, A. C. (1998). *J. Struct. Biol.* **123**, 248–259.
Bochtler, M., Ditzel, L., Groll, M., Hartmann, C. & Huber, R. (1999). *Annu. Rev. Biophys. Biomol. Struct.* **28**, 295–317.
Bochtler, M., Hartmann, C., Song, H. K., Bourenkov, G. P., Bartunik, H. D. & Huber, R. (2000). *Nature (London)*, **403**, 800–805.
Bolon, D. N., Wah, D. A., Hersch, G. L., Baker, T. A. & Sauer, R. T. (2004). *Mol. Cell*, **13**, 443–449.
Brunger, A. T. *et al.* (1998). *Acta Cryst.* D**54**, 905–921.
Chien, P., Grant, R. A., Sauer, R. T. & Baker, T. A. (2007). *Structure*, **15**, 1296–1305.
Chien, P., Perchuk, B. S., Laub, M. T., Sauer, R. T. & Baker, T. A. (2007). *Proc. Natl. Acad. Sci. USA*, **104**, 6590–6595.
Donaldson, L. W., Wojtyra, U. & Houry, W. A. (2003). *J. Biol. Chem.* **278**, 48991–48996.
Dougan, D. A., Weber-Ban, E. & Bukau, B. (2003). *Mol. Cell*, **12**, 373–380.
Flynn, J. M., Levchenko, I., Sauer, R. T. & Baker, T. A. (2004). *Genes Dev.* **18**, 2292–2301.
Flynn, J. M., Levchenko, I., Seidel, M., Wickner, S. H., Sauer, R. T. & Baker, T. A. (2001). *Proc. Natl. Acad. Sc.i USA*, **98**, 10584–10589.
Flynn, J. M., Neher, S. B., Kim, Y. I., Sauer, R. T. & Baker, T. A. (2003). *Mol. Cell*, **11**, 671–683.
Frank, E. G., Ennis, D. G., Gonzalez, M., Levine, A. S. & Woodgate, R. (1996). *Proc. Natl. Acad. Sci. USA*, **93**, 10291–10296.
Goldberg, A. L. (1990). *Semin. Cell Biol.* **1**, 423–432.
Goldberg, A. L. (2003). *Nature (London)*, **426**, 895–899.
Gottesman, S. (1996). *Annu. Rev. Genet.* **30**, 465–506.
Gottesman, S., Roche, E., Zhou, Y. & Sauer, R. T. (1998). *Genes Dev.* **12**, 1338–1347.
Grimaud, R., Kessel, M., Beuron, F., Steven, A. C. & Maurizi, M. R. (1998). *J. Biol. Chem.* **273**, 12476–12481.
Hanson, P. I. & Whiteheart, S. W. (2005). *Nat. Rev. Mol. Cell Biol.* **6**, 519–529.
Hershko, A. & Ciechanover, A. (1998). *Annu. Rev. Biochem.* **67**, 425–479.
Keiler, K. C., Waller, P. R. & Sauer, R. T. (1996). *Science*, **271**, 990–993.
Kessel, M., Wu, W., Gottesman, S., Kocsis, E., Steven, A. C. & Maurizi, M. R. (1996). *FEBS Lett.* **398**, 274–278.
Kim, D. Y. & Kim, K. K. (2003). *J. Biol. Chem.* **278**, 50664–50670.
Lessner, F. H., Venters, B. J. & Keiler, K. C. (2007). *J. Bacteriol.* **189**, 272–275.
Levchenko, I., Grant, R. A., Flynn, J. M., Sauer, R. T. & Baker, T. A. (2005). *Nat. Struct. Mol. Biol.* **12**, 520–525.
Levchenko, I., Grant, R. A., Wah, D. A., Sauer, R. T. & Baker, T. A. (2003). *Mol. Cell*, **12**, 365–372.
Levchenko, I., Luo, L. & Baker, T. A. (1995). *Genes Dev.* **9**, 2399–2408.
Levchenko, I., Seidel, M., Sauer, R. T. & Baker, T. A. (2000). *Science*, **289**, 2354–2356.
McGinness, K. E., Baker, T. A. & Sauer, R. T. (2006). *Mol. Cell*, **22**, 701–707.
Mayer, B. J. & Eck, M. J. (1995). *Curr. Biol.* **5**, 364–367.
Mogk, A., Dougan, D., Weibezahn, J., Schlieker, C., Turgay, K. & Bukau, B. (2004). *J. Struct. Biol.* **146**, 90–98.
Neher, S. B., Flynn, J. M., Sauer, R. T. & Baker, T. A. (2003). *Genes Dev.* **17**, 1084–1089.
Neher, S. B., Sauer, R. T. & Baker, T. A. (2003). *Proc. Natl. Acad. Sci. USA*, **100**, 13219–13224.
Park, E. Y., Lee, B. G., Hong, S. B., Kim, H. W., Jeon, H. & Song, H. K. (2007). *J. Mol. Biol.* **367**, 514–526.
Pines, J. & Lindon, C. (2005). *Nat. Cell Biol.* **7**, 731–735.
Sauer, R. T. *et al.* (2004). *Cell*, **119**, 9–18.
Schwede, T., Kopp, J., Guex, N. & Peitsch, M. C. (2003). *Nucleic Acids Res.* **31**, 3381–3385.
Song, H. K. & Eck, M. J. (2003). *Mol. Cell*, **12**, 75–86.
Song, H. K., Hartmann, C., Ramachandran, R., Bochtler, M., Behrendt, R., Moroder, L. & Huber, R. (2000). *Proc. Natl. Acad. Sci. USA*, **97**, 14103–14108.
Thibault, G., Tsitrin, Y., Davidson, T., Gribun, A. & Houry, W. A. (2006). *EMBO J.* **25**, 3367–3376.
Thibault, G., Yudin, J., Wong, P., Tsitrin, V., Sprangers, R., Zhao, R. & Houry, W. A. (2006). *Proc. Natl. Acad. Sci. USA*, **103**, 17724–17729.
Wah, D. A., Levchenko, I., Baker, T. A. & Sauer, R. T. (2002). *Chem. Biol.* **9**, 1237–1245.
Wah, D. A., Levchenko, I., Rieckhof, G. E., Bolon, D. N., Baker, T. A. & Sauer, R. T. (2003). *Mol. Cell*, **12**, 355–363.
Wickner, S., Maurizi, M. R. & Gottesman, S. (1999). *Science*, **286**, 1888–1893.
Withey, J. H. & Friedman, D. I. (2002). *Curr. Opin. Microbiol.* **5**, 154–159.
Wojtyra, U. A., Thibault, G., Tuite, A. & Houry, W. A. (2003). *J. Biol. Chem.* **278**, 48981–48990.
Zhou, Y., Gottesman, S., Hoskins, J. R., Maurizi, M. R. & Wickner, S. (2001). *Genes Dev.* **15**, 627–637.